Motivation, rationale and key results from the GERBILS Saharan dust measurement campaign

J. M. Haywood,[a,b*†] B. T. Johnson,[a] S. R. Osborne,[a] A. J. Baran,[a] M. Brooks,[a] S. F. Milton,[a] J. Mulcahy,[a] D. Walters,[a] R. P. Allan,[c] A. Klaver,[d] P. Formenti,[d] H. E. Brindley,[e] S. Christopher[f] and P. Gupta[g]

[a] *Met Office, Exeter, UK*
[b] *College of Engineering, Mathematics, and Physical Science, Exeter University, UK*
[c] *Department of Meteorology, University of Reading, UK*
[d] *Laboratoire Interuniversitaire des Systèmes Atmosphériques (LISA), CNRS, Université Paris Est Créteil et Université Paris Diderot, Créteil, France*
[e] *Imperial College, London, UK*
[f] *Department of Atmospheric Science, University of Alabama, Huntsville, Alabama, USA*
[g] *University of Maryland Baltimore County, NASA GSFC, Greenbelt, Maryland, USA*

*Correspondence to: J. Haywood, Met Office OBR, FitzRoy Road, Exeter EX1 3PB, UK.
E-mail: jim.haywood@metoffice.gov.uk

The Geostationary Earth Radiation Budget Intercomparison of Longwave and Shortwave radiation (GERBILS) was an observational field experiment over North Africa during June 2007. The campaign involved 10 flights by the FAAM BAe-146 research aircraft over southwestern parts of the Sahara Desert and coastal stretches of the Atlantic Ocean. Objectives of the GERBILS campaign included characterisation of mineral dust geographic distribution and physical and optical properties, assessment of the impact upon radiation, validation of satellite remote sensing retrievals, and validation of numerical weather prediction model forecasts of aerosol optical depths (AODs) and size distributions. We provide the motivation behind GERBILS and the experimental design and report the progress made in each of the objectives. We show that mineral dust in the region is relatively non-absorbing (mean single scattering albedo at 550 nm of 0.97) owing to the relatively small fraction of iron oxides present (1–3%), and that detailed spectral radiances are most accurately modelled using irregularly shaped particles. Satellite retrievals over bright desert surfaces are challenging owing to the lack of spectral contrast between the dust and the underlying surface. However, new techniques have been developed which are shown to be in relatively good agreement with AERONET estimates of AOD and with each other. This encouraging result enables relatively robust validation of numerical models which treat the production, transport, and deposition of mineral dust. The dust models themselves are able to represent large-scale synoptically driven dust events to a reasonable degree, but some deficiencies remain both in the Sahara and over the Sahelian region, where cold pool outflow from convective cells associated with the intertropical convergence zone can lead to significant dust production. Copyright © 2011 Royal Meteorological Society and British Crown Copyright, the Met Office

Key Words: Saharan dust; mineral dust; airborne measurements; remote sensing

Received 18 November 2010; Revised 25 January 2011; Accepted 28 January 2011; Published online in Wiley Online Library 8 June 2011

Citation: Haywood JM, Johnson BT, Osborne SR, Baran AJ, Brooks M, Milton SF, Mulcahy J, Walters D, Allan RP, Klaver A, Formenti P, Brindley HE, Christopher S, Gupta P. 2011. Motivation, rationale and key results from the GERBILS Saharan dust measurement campaign. *Q. J. R. Meteorol. Soc.* **137**: 1106–1116. DOI:10.1002/qj.797

1. Motivation and rationale for the experiment

The radiative impacts of mineral dust have come under increased scrutiny over the last decade as mineral dust can have a profound local, regional, and continental-scale impact on both top of atmosphere and surface fluxes in both solar and terrestrial regions of the electromagnetic spectrum. Three key measurement campaigns and modelling projects that motivated the GERBILS campaign are summarised here.

The SaHAran Dust Experiment (SHADE; Tanré *et al.*, 2003) investigated the impacts on the radiation budget over the ocean off the coast of West Africa. Haywood *et al.* (2003) showed a clear increase in the reflected solar radiation by mineral dust of up to 130 W m^{-2} for a mineral dust aerosol optical depth (AOD) at 550 nm (AOD$_{550}$) of around 1.5. Retrievals of the solar direct radiative impact were found to be in good agreement with those derived from the Clouds and the Earth's Radiant Energy System (CERES) satellite instrument. Simultaneous investigations of the terrestrial impact of Saharan dust using a high spectral resolution interferometer revealed a strong signature in the 8–12 μm atmospheric window with a brightness temperature reduction in zenith observations of up to 30 K (Highwood *et al.*, 2003).

The SINERGEE (SImulations from an NWP model to Exploit Radiation data from a new Geostationary satellite, Explore radiative processes and Evaluate models) project has provided an extremely useful insight into the performance of the global numerical weather prediction (NWP) configuration of the Met Office Unified Model^{TM} (MetUM) in terms of the top of the atmosphere outgoing long wave (LW) and short wave (SW) radiation budget (Allan *et al.*, 2005). This project highlighted a large discrepancy in the clear-sky outgoing LW radiation (OLRc) over the Sahara Desert, which reaches a maximum during the June–July–August period each year (Haywood *et al.*, 2005). An example of the OLRc anomaly is shown in Figure 1 when comparing the MetUM to both the Meteosat-7 narrow band and preliminary measurements from the first Geostationary Earth Radiation Budget Experiment (GERB) instrument (Harries *et al.*, 2005) onboard Meteosat-8.

Very similar geographical features can be seen in both sets of analyses, with the largest discrepancy in the OLRc exceeding 50 W m^{-2}. Haywood *et al.* (2005) suggested that the most likely explanation for the overestimation of OLRc in the MetUM was the lack of mineral dust: when the radiative effects of mineral dust derived from the Total Ozone Mapping Spectrometer (TOMS) were included, the discrepancy was reduced.

Comprehensive observations of both mineral dust and biomass burning aerosol were performed during the Dust and Biomass burning Experiment (DABEX; Haywood *et al.*, 2008), a project affiliated with the overarching African Monsoon Multidisciplinary Analysis (AMMA; Lebel *et al.*, 2010), when the aircraft was based in Niamey, Niger. The radiative impacts of aerosols were shown to be significant both at the surface and at the top of the atmosphere in a number of measurements. For example, Haywood *et al.* (2008) used data from the Atmospheric Radiation Measurement (ARM) Mobile Facility (AMF) to show a decrease in the peak surface SW irradiance by around 230 W m^{-2} when the combined mineral dust and biomass burning AOD$_{550}$ increased by around 1. Milton *et al.* (2008) performed a seasonal analysis of model *versus* AMF measurements for January–February–March 2006 and found a mean daytime SW impact from mineral dust and biomass burning aerosol in excess of 80 W m^{-2}. Milton *et al.* (2008) show that around 40% of this bias is due to dust in January, but greater than 90% of this bias is due to dust by mid March. Johnson *et al.* (2009) used aircraft instrumentation to measure instantaneous reductions in near-surface SW radiation owing to biomass burning and mineral dust aerosols of around 150 W m^{-2} in the vicinity of Niamey, Niger.

These three projects suggest that mineral dust exerts a very significant perturbation to the radiation budget in both the SW and LW regions of the spectrum, and that the neglect of the radiative impacts of mineral dust in NWP models causes a significant bias in the radiation budget, with consequences on the atmospheric and surface heating rates which influence the dynamical evolution of such models. Mineral dust will increase the absorption of both SW and LW radiation in the atmosphere, and decrease the SW flux at the surface while increasing the LW flux at the surface. The diurnal cycle is likely to be influenced owing to LW effects acting throughout the day, while SW impacts only act during daylight (e.g. Parker *et al.*, 2005). Milton *et al.* (2008) modelled the overall impact of mineral dust during a Saharan dust event and found that dust exerts a net atmospheric warming and a surface cooling which increases the static stability of the atmosphere.

While these three projects noted above give insight into the physical and radiative properties of mineral dust, no dedicated investigation of mineral dust had been carried out during the summer months over land surfaces close to the sources of mineral dust. The intense heating surface and absence of biomass burning aerosols during summer months will lead to a very different dynamical environment, and the lack of complex interactions between mineral dust and biomass burning aerosols (e.g. Capes *et al.*, 2008) will lead to a more straightforward assessment of the physical and radiative properties of mineral dust. Hence the GERBILS intensive airborne measurement campaign was justified with the following objectives:

1. To characterise the geographic distribution and physical and optical properties of mineral dust
2. To assess the impacts of mineral dust on the radiative budget
3. To assess satellite retrievals of mineral dust associated radiative impacts
4. To use the aircraft and satellite remote sensing techniques to validate and improve the performance of dust modelling within numerical models

2. Pre-campaign experimental design and flight patterns

The representivity of the OLRc bias shown July 2003 in Figure 1 was investigated before deployment of the aircraft by examining the inter-annual variability throughout the June–July–August 2003–2005 period. Although some inter-annual differences in the position and the magnitude of the OLRc biases were found, the area of maximum OLRc bias was found to occur consistently at a latitude of 15–20°N and a longitude of 10°W–5°E (see Allan *et al.*, 2011). An idea to use two bases – one to the east (Niamey, Niger) and one to the west (Nouakchott, Mauritania) – was developed so that the aircraft could approach, pass over, and depart

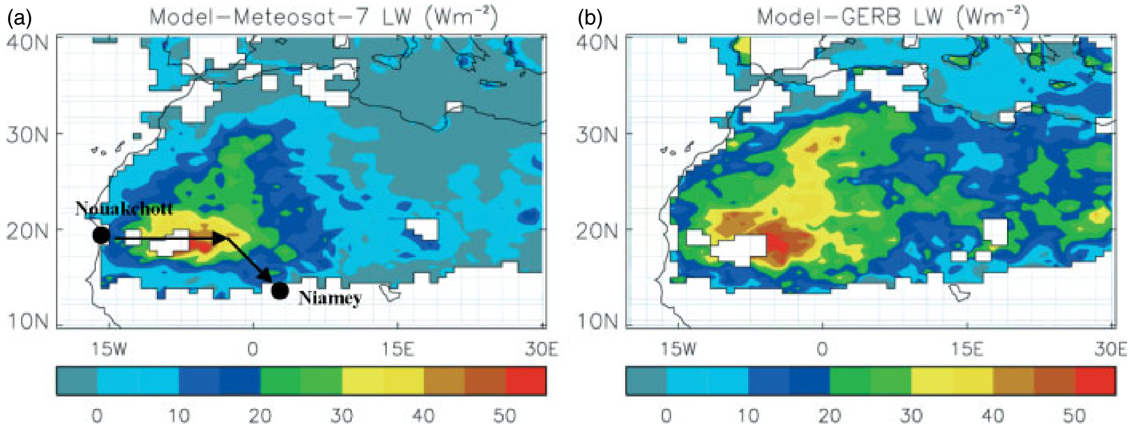

Figure 1. An example of the OLR anomaly (from July 2003) when comparing the UM against (a) that from Meteosat 7, (b) the GERB instrument on Meteosat 8. The positions of Nouakchott (Mauritania) and Niamey (Niger) are marked in (a), together with a 'standard route' that was flown by the aircraft as described in the text.

Table I. The flying plan developed for GERBILS. 'Standard route' indicates flights along 18°N as described in the text. The comments show deviations from the standard route. Nouakchott and Niamey airfields are at 18.10°N, 15.94°W 2.18°N, and 13.48°E respectively.

Date	Planned flight activity	Comments
18/06/07	UK → Nouakchott	B294: Flight over ocean refuelling at Agadir
19/06/07	Nouakchott → Niamey	B295: Standard route
20/06/07	Set-up (NO FLYING)	NO FLYING
21/06/07	Niamey → Nouakchott	B296: Diverted to south to intercept dust plume.
22/06/07	Nouakchott → Niamey	B297: Flight over ocean to intercept dust plume. B298: Direct routing to Niamey.
23/06/07	Down day (NO FLYING)	NO FLYING
24/06/07	Niamey → Nouakchott	B299: Standard route
25/06/07	Nouakchott → Niamey	B300: Standard route
26/06/07	Down day (NO FLYING)	NO FLYING
27/06/07	Niamey → Nouakchott	B301: Standard route
28/06/07	Nouakchott → Niamey	B302: Standard route
29/06/07	Niamey → UK	B303: High altitude only

from the area with maximum OLRc bias. An intensive fixed flying programme was developed where the destination of the aircraft on a particular day was predetermined (Table I).

While the proposed fixed flying programme could simplify logistics, a study of the effectiveness of such a stringent programme was performed before deployment. For effective radiation measurements to be made, the aircraft would have to operate in cloud-free conditions away from the presence of any cloud. We utilise the satellite analysis of Allan *et al.* (2011) to determine cloudy and cloud-free pixels: cloud-free pixels are only assigned if cloud cover is determined to be less than 1% by Meteosat. Table II shows the likelihood of encountering 0–6 cloud-free days during the 6 days associated with the three pairs of Niamey ↔ Nouakchott flights using data from the GERB satellite for June–August for the years 2003–2005.

There is a better than 85%–63%–36% chance of experiencing at least 3–4–5 cloud-free days, respectively. The mean OLRc bias is in excess of 20 W m^{-2}. The fractional number of pixels with less than 1% cloud cover exceeds 40% for the majority of the time. Given these statistics, this fixed flying programme appeared reasonable. A flight pattern following a 'standard route' along 18°N was devised, routing the aircraft through areas statistically expected to have the highest OLRc bias (see Figure 1). Table I shows that while the 'standard route' at 18°N was followed for the majority of the flights, some flexibility in the flying programme was possible provided the aircraft destination airport was adhered to. This allowed diversion of the aircraft to the south of the region and over ocean when a significant dust event occurred. The geographic distribution of flight patterns for the campaign is shown in Johnson and Osborne (2011).

Because the distance between Niamey and Nouakchott is large (over 2000 km as a direct routing) compared to the range of the BAe-146 aircraft, only a little flexibility was allowed in the flight patterns. A schematic diagram of a typical flight plan is shown in Figure 2. Because the range of the aircraft decreases with decreasing altitude the aircraft could not fly at low altitudes ($<$5 km) for the entire flight and spent major portions of each flight at altitudes of 7–8 km, remotely sensing the dust and desert surface from above. Time spent travelling on a reciprocal heading was also limited to about 15–20 minutes. These constraints were tighter when travelling from Nouakchott to Niamey owing to the headwind which European Centre Re-Analysis (ERA40) suggested was around 10 m s^{-1} at 600 hPa.

Typically on the 'standard route' the aircraft performed straight and level runs at FL200–FL250 (7–8 km) above the aerosol, dropping radiosondes to measure the temperature, humidity, and wind speed and direction. These data were assimilated within the MetUM, providing high-resolution,

Table II. The fractional number of cloud-free days that might be expected using the proposed flying schedule. Data from June–August are used for the 3 years 2003–2005 in the calculations along a line from Niamey to Nouakchott. A cloud-free day is defined as one where cloud cover in a Meteosat pixel is less than 1%.

No. of cloud-free days	0	1	2	3	4	5	6
Likelihood cloud-free % (cumulative)	0	4% (100%)	11% (96%)	22% (85%)	27% (63%)	27% (36%)	9% (9%)
OLRc bias (W m^{-2}) mean and (SD)	0	19 (11)	28 (11)	25 (8)	24 (8)	25 (8)	24 (7)
% pixels cloud free	0	21	41	41	43	46	46

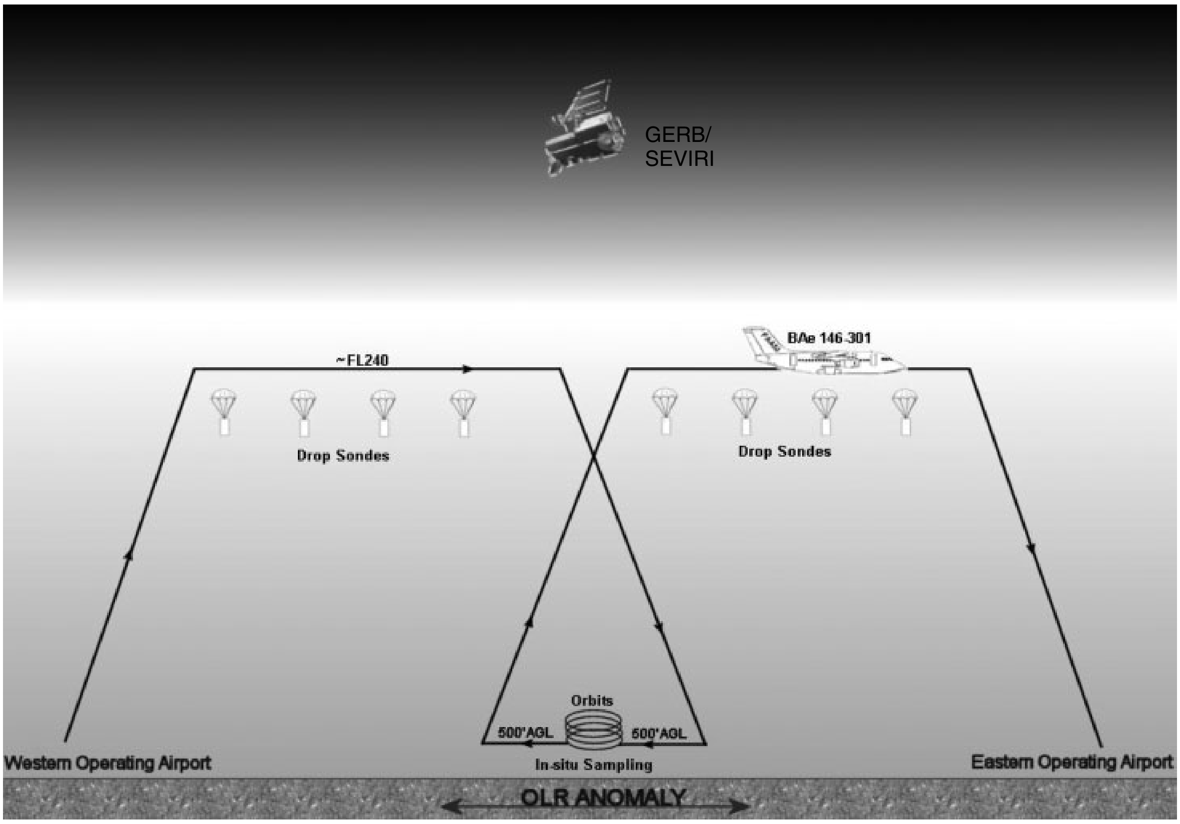

Figure 2. A sample flight plan from the western operating airport (Nouakchott) to the eastern operating airport (Niamey).

high-quality temperature, humidity and wind-field data in a geographically data-sparse area. Upon approaching an area of heavy dust loading as determined from satellite data and from model forecasts, the aircraft performed a profile down into the mineral dust, a low-level straight and level run, and a series of banked orbits to make measurements analogous to the almucantar scans of AERONET (see Osborne *et al.*, 2011), before profiling back up and continuing at FL200–FL250 (7–8 km) to the destination airport. Nevertheless, these flight patterns proved very effective at sampling peak concentrations of mineral dust aerosol.

3. Flight planning during the GERBILS campaign

It was important during GERBILS to ensure that the aircraft low-level work (see Figure 2) was performed under dusty conditions. Throughout the campaign, two main tools were used to aid with flight planning and to co-ordinate the low-level work of the aircraft: satellite images, in particular the EUMETSAT Spinning Enhanced Visible and Infrared Imager (SEVIRI) RGB dust product, and forecasts from the Crisis Area Mesoscale model (CAM, Greed *et al.*, 2008; Johnson *et al.*, 2011).

The SEVIRI dust product is available every 15 minutes and colours blue the 10.8 μm channel, red the difference between the 12.0 and 10.8 μm channels, and green the difference between the 10.8 and 8.7 μm channels. This product strongly emphasizes high atmospheric loadings of mineral dust that, in the absence of cloud, lead to magenta (pink) colours in the images. The product has therefore been used for studying the development and propagation of dust storms at high temporal resolution (e.g. Slingo *et al.*, 2006; Milton *et al.*, 2008). The sequence of SEVIRI RGB dust products at 1230 UTC each day is shown in Figure 3 together with the flight patterns.

Dust events are clearly evident, particularly during the first half of the campaign. A large dust event centred on the Hoggar Mountains in southern Algeria is evident on 18 June which progresses south and westwards. On 20 June (not shown) the large synoptic-scale dust storm reinvigorates and plunges south in a trough associated with the African easterly waves and the intertropical convergence zone (ITCZ) and

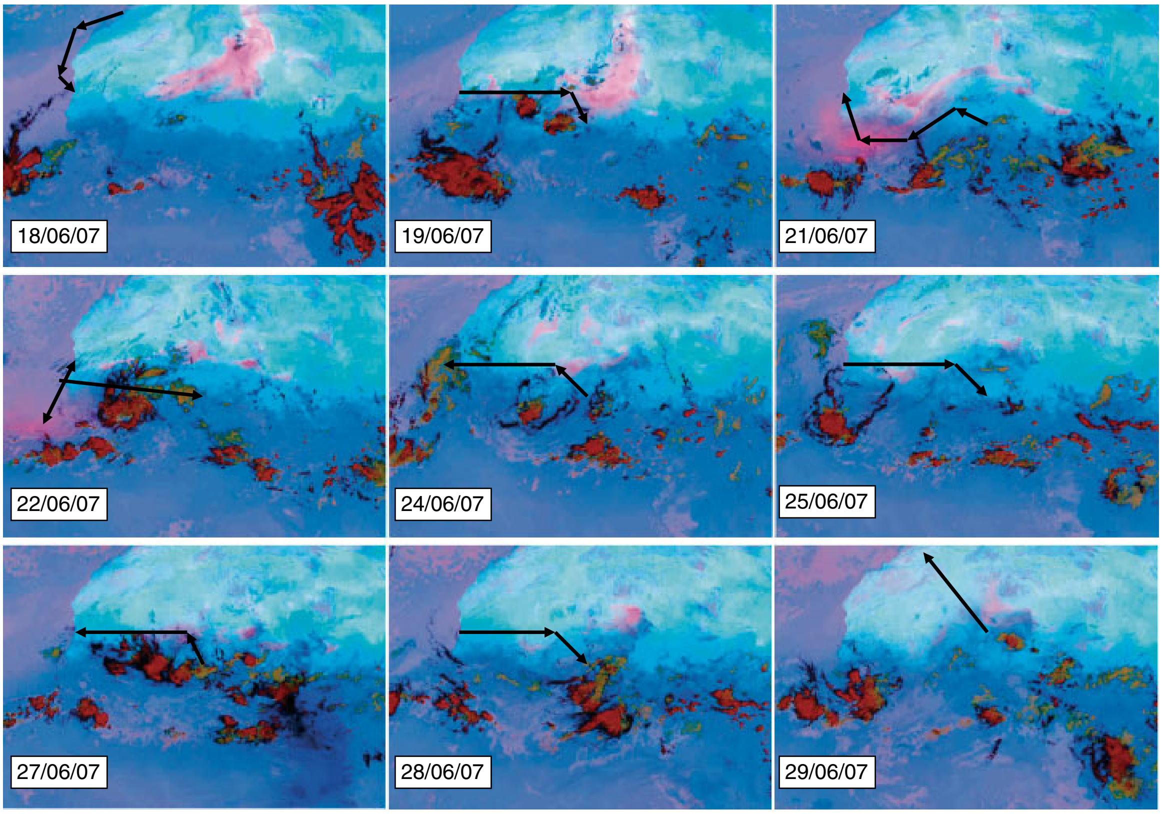

Figure 3. The SEVIRI RGB dust products at 1230 UTC throughout the GERBILS measurements period. Only days with flights are shown. The dust is shown by the intense pink colours, while deep convective clouds associated with the ITCZ are shown in brown. The approximate route of the aircraft is shown by the arrows (see Johnson and Osborne, 2011) for more details.

is then advected out over the Atlantic Ocean on 21 and 22 June. Subsequent synoptic-scale mineral dust activity is reduced as the monsoon flow and deep convective clouds associated with the ITCZ move to the north. However, while synoptic-scale generation and transport of dust are reduced in the second half of the GERBILS period, dust continues to be produced at smaller scales. Marsham *et al.* (2008) analyse GERBILS flight data from 27 June and show that significant dust is generated by the nocturnal monsoon winds (Parker *et al.*, 2005) and cold pool outflow from deep convective systems of the ITCZ.

The CAM model is a limited area configuration of the MetUM run at 12–20 km resolution over a relocatable domain. For GERBILS, the CAM is run at 20 km with 38 vertical levels over a domain approximately covering 7°S–37°N, 45°W–20°E, with boundary conditions supplied by the global version of the MetUM. Both the CAM and global MetUM configurations were used in DABEX for forecasting dust generation, advection, and deposition (Greed *et al.*, 2008; Milton *et al.*, 2008). Figure 4 shows the AOD_{550} forecast by the CAM model during the campaign when flights occurred.

Generally, there is a reasonable spatial correlation between the areas where the SEVIRI RGB dust product show significant dust (see Figure 3) with the areas of high AOD_{550}. The geographic progression of the large dust storm indicated in the SEVIRI RGB product on 21–22 June appears reasonably well represented. The CAM forecast was the main tool leading to the decision to divert the aircraft from the 'standard route' to that shown in Figure 3 for 21–22 June, a decision that was later vindicated by the SEVIRI RGB products. A full description of the CAM model and its performance in terms of the AOD and size distribution when compared against a wide range of satellite and *in situ* measurements is provided by Johnson *et al.* (2011), as will be summarised in section 5.4.

4. Aircraft instrumentation and satellite products

The FAAM BAe146 is jointly funded by the Met Office and the Natural Environment Research Council (NERC), and has the largest payload of the European fleet of meteorological research aircraft. The scientific payload was tailored for aerosol, radiation/remote sensing and basic gas phase chemistry measurements as well as measurements of standard meteorological variables such as temperature, humidity, and wind speed and direction. Aircraft instrumentation was a stripped down version of that used during the DABEX campaign, which is fully described in Haywood *et al.* (2008) and at http://www.faam.ac.uk/index.php/science-instruments; only a brief description of relevant instrumentation is given here.

The size distribution of mineral dust over the size range 0.05–30 μm radius was determined using a combination of the wing-mounted Passive Cavity Aerosol Spectrometer Probe (PCASP-100X) and a second version of the Small Ice Detector (SID2; Cotton *et al.*, 2010). Corrections were made for refractive index by assuming the refractive index of Balkanski *et al.* (2007) with a haematite content of 1.5%, and shape by assuming irregular shaped particles and using combinations of Mie scattering, T-matrix, and ray tracing techniques (Johnson and Osborne, 2011). A standard Rosemount inlet fed the internally mounted TSI 3563

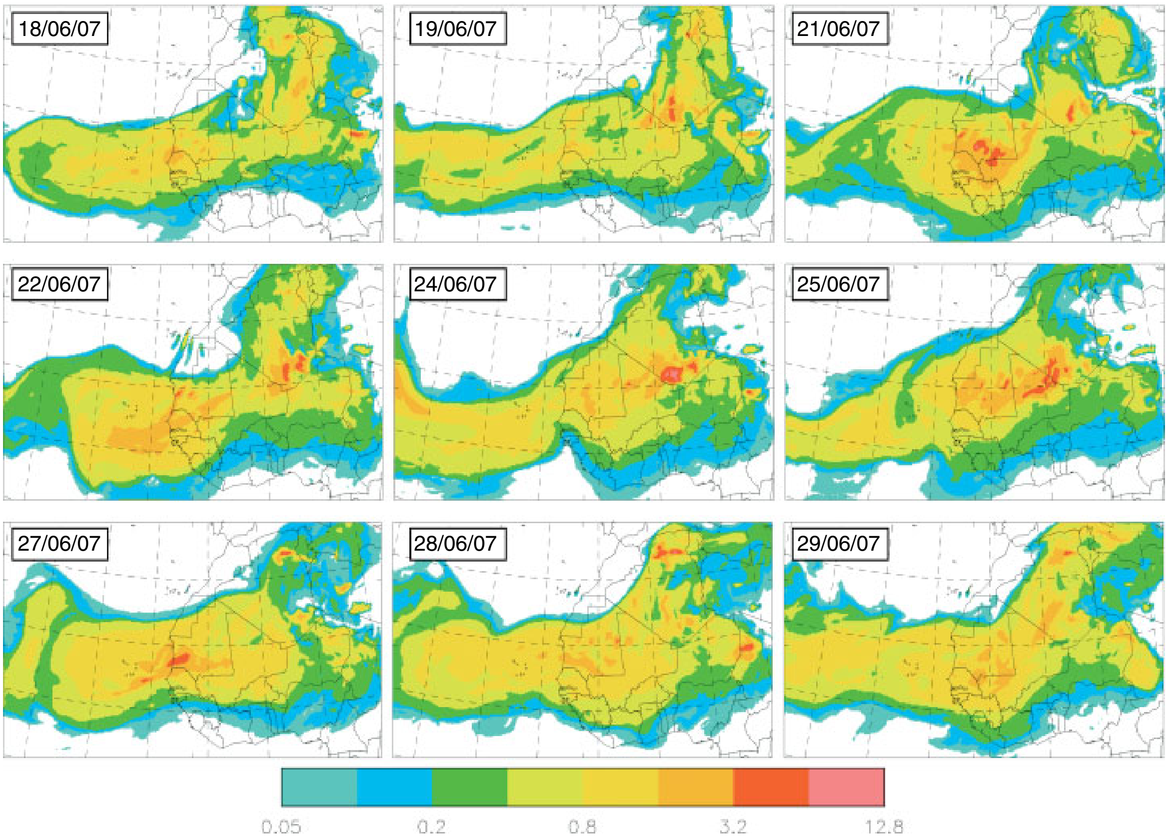

Figure 4. The AOD_{550} predicted by the operational version of the CAM configuration of the MetUM.

3-wavelength nephelometer and particle soot absorption photometer (PSAP), which were corrected for non-ideal scattering (Anderson and Ogren, 1998), and absorption artefacts (Bond *et al.*, 1999). The filter measurement system (Klaver *et al.*, 2011) consists of thin-walled nozzles (Andreae *et al.*, 1998) with curved leading edges leading to two stacked filter units under sub-isokinetic conditions. Each stacked filter unit consisted of a Nucleopore filter of 47 mm diameter and nominal pore size 0.4 μm. Gas phase measurements were made using Rosemount inlets coupled to a TECO 42 for measuring NO and NO_2, a TECO 43C for measuring SO_2 and a TECO 49 for measuring ozone, while CO was measured using an Aero-laser AL5002.

Radiation measurements were made using upper and lower clear-dome and red-dome Eppley pyranometers (e.g. Haywood *et al.*, 2003) to measure the 0.3–3.0 and 0.7–3.0 μm irradiances respectively. Spectrally resolved upward and downward irradiances at a resolution of up to 0.0032 μm were determined from the Solar Hemispheric Integrating Measurement System (SHIMS), which consists of an integrating head coupled by fibre optics to Zeiss spectrometer units. A new 'pirouette' correction procedure detailed by Haywood *et al.* (2011) was applied to account for pitch and roll variations for downwelling irradiances, while no correction was deemed necessary for upwelling irradiances. Spectral radiances at the same spectral resolution as SHIMS were also measured using a pointable narrow field of view short-wave spectrometer (SWS). As well as zenith and nadir measurements, aircraft orbits where the aircraft was flown in a circle at a fixed angle of bank enabled the spectral radiances to be measured as a function of scattering angle (Osborne *et al.*, 2011). Such a procedure provides data analogous to the almucantar scans from the Aerosol Robotic Network (AERONET; e.g. Dubovik *et al.*, 2006). The Airborne Research Interferometer Evaluation System (ARIES) was also flown and has previously been used to measure the spectrally resolved impact of mineral dust in the long-wave region of the spectrum at a spectral resolution of approximately 0.5 cm^{-1} (Highwood *et al.*, 2003).

A wide range of satellite instruments and data were used in pre-campaign planning (section 2), flight planning during the campaign (section 3) or in post-campaign quantitative analyses of AOD or mineral dust radiative effects (section 5); those relied on most heavily are summarised in Table III.

5. Key results

The GERBILS measurement campaign had four major objectives (section 1). Here we discuss the progress made in each of these objectives and the key results.

5.1. *Aircraft-based assessments of the geographical distribution and physical and optical properties of mineral dust*

Aircraft-mounted filter measurements of the chemical composition of mineral dust were examined by Klaver *et al.* (2011), while the geographic distribution and physical and optical properties were examined in detail by the aircraft-mounted measurements of Johnson and Osborne (2011). Filters exposed on the aircraft (Klaver *et al.*, 2011) were analysed by X-ray diffraction techniques, which indicated that clays such as illite and kaolinite made up 80–90% of the aerosol mass, while quartz, calcite, dolomite, gypsum, alkali feldspars and iron oxides made up the remaining mass. Iron oxides, which are responsible for the

Table III. Summary of the satellite instruments and products that were used in operational planning or scientific analyses for GERBILS.

Satellite sensor	Use during GERBILS
GERB[a]	Diagnosis of difference between model OLRc and observations to determine dust radiative impact (Allan *et al.*, 2011)
MODIS[b]	Operational determination of dust storms using rapid response data (http://rapidfire.sci.gsfc.nasa.gov/subsets/) Standard AOD (Remer *et al.*, 2005) and Deep Blue AOD (Hsu *et al.*, 2006) utilised over bright surfaces: Christopher *et al.* (2008, 2009, 2011)
MISR[c]	Used as standard to calibrate wide swath OMI retrievals (Christopher *et al.*, 2008, 2009)
OMI[d]	Operational determination of dust storms Correlative relationships developed (Christopher *et al.*, 2008, 2009, 2011) to allow model validation (Johnson *et al.*, 2011)
SEVIRI[e]	Operational RGB product for monitoring dust storms in near-real-time for flight planning. Assessment of dust direct radiative effect (Haywood *et al.*, 2011) Assessment of dust model performance (Johnson *et al.*, 2011)

[a] Geostationary Earth Radiation Budget (Harries *et al.*, 2005).
[b] Moderate Resolution Imaging Spectrometer (Kaufmann *et al.*, 1997).
[c] Multiangle Imaging Spectroradiometer (Khan *et al.*, 2005).
[d] Ozone-monitoring instrument (Torres *et al.*, 2007).
[e] Spinning Enhanced Visible and Infrared Imager (Brindley and Russell, 2008).

majority of absorption of solar radiation, were derived by chemical extraction methods to be 1–3% of the total aerosol mass. This is in the range of values also found by Formenti *et al.* (2008) and Kandler *et al.* (2009) for near-emission and transported dust during DABEX, Dust Outflow and Deposition to the Ocean (DODO) and Saharan Mineral Dust Experiment (SAMUM) measurement campaigns. Klaver *et al.* (2011) also derived the median aspect ratios for mineral dust particles of around 1.5–1.6, similar to those derived by Chou *et al.* (2008) and Kandler *et al.* (2009) for the AMMA/DABEX and SAMUM measurement campaigns.

The AOD derived by integrating the aerosol scattering from the nephelometer during aircraft profiles compared well to that derived from sun photometers located at Nouakchott and Banizoumbou – a surprising result given the suspected low sampling inefficiency of the Rosemount inlet to coarse aerosols when the instrument was installed on the C-130 aircraft (e.g. Haywood *et al.*, 2003). The aircraft measurements suggest that AODs in this data-sparse region are at least as high as current satellite products suggest (Christopher *et al.*, 2009).

The size distribution showed a peak mass concentration at a radius of around 2 μm, in reasonable agreement with the results of SHADE (Haywood *et al.*, 2003) and DABEX (Osborne *et al.*, 2008). The GERBILS size distributions are also remarkably similar to those derived from AERONET retrievals. However, the peak size distribution is significantly smaller than the aircraft observations made during SAMUM (Weinzierl *et al.*, 2008). The differences between SAMUM and GERBILS size distributions could be due to a combination of factors, including differences in instrumentation, measurement techniques and instrument corrections, and differences in geographic region (SAMUM was based in northwest Sahara). Differences in underlying soil types and surface conditions may affect the emitted size distribution of mineral dust and due to sedimentation the measured size distribution varies with distance from the source region.

The absorption from the mineral dust as measured using the corrected nephelometer and PSAP combination suggests single scattering albedos at 550 nm (SSA_{550}) in the range 0.92–0.99, with a mean of 0.97. Johnson and Osborne (2011) show that the mineral dust refractive indices from Balkanski *et al.* (2007) assuming 1.5% haematite gave reasonable agreement with the single scattering albedo, consistent with the findings of Klaver *et al.* (2011). An SSA_{550} of 0.97 is higher than that obtained from aircraft measurements during the SAMUM experiment performed in Morocco but in reasonable agreement with that from the SAMUM-2 experiment, which made measurements in a similar geographical location to GERBILS (Andreas Petzold, personal communication). Ground-based measurements during SAMUM (Schladitz *et al.*, 2009) estimate the single scattering albedo at Tindouf in northern Morocco to be 0.96 ± 0.02 (at 540 nm) when high concentrations of mineral dust are present, which is similar to our estimates.

5.2. *The impact of mineral dust on radiation and radiative closure*

Osborne *et al.* (2011) used aircraft orbits and SW spectral radiance measurements in close proximity to the Dakar AERONET site (Holben *et al.*, 1998) to show that the aircraft SWS reproduced the AERONET sun photometer radiances as a function of the scattering angle during almucantar scans (e.g. Dubovik *et al.*, 2006). Modelled radiances were then computed for spheres, spheroids, and irregular-shaped particles (polycrystals) with sharp edges using combinations of Mie scattering, T-matrix, and ray tracing diffraction on facet techniques (Havemann and Baran, 2001; Hesse, 2008). While the single scattering albedo showed insignificant variation (Johnson and Osborne, 2011), the scattered phase function and scattered radiance are particularly sensitive to the particle shape (Osborne *et al.*, 2011). Kokhanovsky (2003) performed laboratory studies showing that irregular polycrystals can represent scattered radiances from mineral dust to high accuracy. However, Osborne *et al.* (2011) are the first to show that use of polycrystals definitively leads to better agreement between measured and modelled atmospheric radiances than the use of spheres or spheroid models (i.e. models with smooth surfaces) for high optical depth mineral dust aerosol. These results indicate that some form of irregularity and/or surface roughness is required if the scattering phase function is to be adequately modelled. Clearly, there is a need for further research and field measurements in this area, particularly at backscattering angles, where differences in scattering are manifest between smooth and irregular particles. Osborne *et al.* (2011) also show that while the SW spectral signature of mineral dust is clearly detectable in low-altitude zenith measurements over land, there are significant difficulties in detection in high-altitude nadir measurements owing to the variability in the underlying surface reflectance. The aircraft measurements and radiative transfer modelling suggest that daytime mean reductions of downwelling SW radiation at the surface are estimated to be 137–153 W m^{-2}/AOD_{550}. In the LW, the peak reduction in the brightness temperature in high-altitude nadir data for a relatively modest AOD_{550} of around 0.8 was 14 K, which corresponded to a reduction in OLRc by 14–26 W m^{-2} at local noon depending on the assumed refractive indices. These values are entirely plausible, given the analysis by Haywood *et al.* (2005) and Allan *et al.* (2011) and match reasonably well with values derived from GERB-like SEVIRI fluxes in the presence of aerosol (Brindley and Russell, 2008). The Balkanski *et al.* (2007) refractive indices appear to perform reasonably in obtaining radiative closure in the LW region of the spectrum (Osborne *et al.*, 2011; Haywood *et al.*, 2011). Osborne *et al.* (2011) suggest a diurnal average LW radiative impact of around 18 W m^{-2}/AOD_{550}.

While the majority of the GERBILS measurement campaign was performed over desert regions, Haywood *et al.* (2011) perform a radiative closure study over ocean regions while the aircraft was on route to the campaign. Haywood *et al.* (2011) clearly detect a significant upwelling SW direct radiative effect of 33 ± 3 W m^{-2}, which is reasonably represented by the SEVIRI retrievals developed by Brindley and Russell (2008). The corresponding measured reduction in the downwelling SW flux was around 47 ± 9 W m^{-2}. When variations in the solar zenith angle are accounted for, SW radiative closure appears reasonable provided a lightly absorbing aerosol model is used (spherical, spheroid, and irregular models coupled with the refractive index of Balkanski *et al.* (2007) yield SSA_{550} of 0.95–0.97), closure is not possible using refractive indices from the World Climate Program (1986). The spectral dependence of the SW and LW radiative impacts are clearly detected, and modelled reasonably, although some discrepancies exist in near-infra wavelengths that may be due to inaccurate representation of the spectral dependence of the sea surface reflectance, and in the 8–12 μm atmospheric window owing to the sensitivity to assumed refractive index.

5.3. Satellite retrievals of dust and their associated radiative impact

One of the motivational studies for performing the GERBILS campaign was that of Haywood *et al.* (2005, Section 1), which demonstrated a significant bias in OLRc between the global NWP MetUM and measurements by the Meteosat-7 satellite (see Figure 1) in July 2003. To establish the representativeness of this study, Allan *et al.* (2011) perform a multi-year seasonal analysis of the bias in SW and LW fluxes when compared to a variety of climate models and show that a significant bias in OLRc (mean ∼9–11 W m^{-2} over the North African region 10–40°N, 20°W–30°E) is present in all of the climate models when compared to a range of satellite retrievals. Some of the climate models include the LW properties of mineral dust and some of them do not. Allan *et al.* (2011) find that the bias in LW fluxes is present in all of them. This suggests that, even if dust radiative effects are included in the models, further attention and refinement of mineral dust LW properties is required in climate models if the LW fluxes are to be accurately modelled. Allan *et al.* (2011) show that in a high-resolution version of the MetUM, when the LW properties of aerosols are fully parameterised, the bias is much reduced (Woodage *et al.*, 2010). Further comparisons of the MetUM against GERB show that the radiative biases were indeed largest during 2003 (Haywood *et al.*, 2005), but that the LW and SW biases had decreased. Allan *et al.* (2011) suggest that the reasons for the decrease in biases are likely a combination of improvements in the model (e.g. changes to the surface emissivity, improvements to data assimilation) rather than any temporal trend in AOD. Additionally, the GERB data produced during 2003 operated under a preliminary processing system, using Meteosat-7 imager data to define scene type, and are therefore considered of lower accuracy than GERB data produced after March 2004. Nevertheless, model biases remain significant: Allan *et al.* (2011) analyse the GERBILS period, finding OLRc biases as high as 20–30 W m^{-2} during daylight hours, which is in line with what might be expected (section 2) and vindicates the experimental design and aircraft deployment (section 3).

The aircraft observations over ocean (Haywood *et al.*, 2011) allow assessment of the SW direct radiative effect derived from SEVIRI (Brindley and Russell, 2008). They show that the agreement between the aircraft observations and the SEVIRI retrievals is encouraging provided the most accurate representations of the bidirectional reflectance function are used. While satellite retrievals over ocean are more straightforward owing to the relative invariance and well-characterised nature of the surface reflectance, retrievals over bright land surfaces are becoming available using a variety of techniques. This is particularly useful as it enables near-source observations where the AODs are at their highest. Christopher *et al.* (2009) presented results from a single case study on 21 June 2007 flight B296 (see Table I) and showed good agreement in the altitude of the aerosol detected by the space-borne CALIPSO lidar when compared to aircraft measurements. Good agreement in remotely sensed AODs from MODIS, MISR and OMI with aircraft measurements was also shown except when the AOD measured by the aircraft was particularly high. Christopher *et al.* (2011) extend the analysis of satellite data from a single case study to the entire GERBILS period. In addition to polar orbiting satellite data, Christopher *et al.* (2011) show the utility of the geostationary SEVIRI data at tracking large-scale dust events as the data are available at 15 minute temporal resolution. AODs over land from MODIS Deep Blue (Hsu *et al.*, 2006), estimated from correlation between OMI and MISR (Christopher *et al.*, 2008), the standard OMI product (Torres *et al.*, 2007), and the SEVIRI sensor (Brindley and Russell, 2008), all show good agreement with those from AERONET sites. MISR is considered a particularly good sensor for making remote sensing retrievals owing to the multi-angle capabilities (Khan *et al.*, 2005), but the narrow swath width makes validation of model fields during short-duration field campaigns such as GERBILS problematic. However, Christopher *et al.* (2011) show correlations between MISR and the other retrievals which agree to within 25%. Taken together, the correlation between broad-swath satellite retrievals and AERONET and broad-swath retrievals and the narrow-swath MISR instrument is encouraging as the broad-swath products can then be used with reasonable confidence to validate models over larger spatial and temporal scales (Haywood *et al.*, 2011; Johnson *et al.*, 2011).

5.4. Validation and improvement in dust modelling

Improving the performance of NWP model simulations of mineral dust was a factor motivating the GERBILS campaign. While the CAM model had been used before in simulating dust production, advection and deposition (Greed *et al.*, 2008), a more comprehensive validation is provided by Johnson *et al.* (2011). Subsequent to the DABEX campaign, the refractive indices of mineral dust were changed from those of the World Climate Program (1986) to those from Balkanski *et al.* (2007) assuming 1.5% haematite content, similar to the 1–3% iron content suggested by Klaver *et al.* (2011). Again, during GERBILS these refractive indices were found to better represent the absorption properties of mineral dust (see Haywood *et al.*, 2011). Two dust uplift schemes were investigated. Johnson *et al.* (2011) found that imposing a log-normal distribution on the emitted size distributions produced a more realistic size distribution when compared to aircraft and AERONET size distributions. Generally, while the dust model provided a reasonable representation of the dust fields (compare Figure 4 with Figure 3), particularly for intense dust events driven by large-scale synoptic-scale meteorology, AODs were found to be on average a factor of 1.5–2.0 too high over the southwest Sahara but 20–50% too low over the Sahel. Untangling the reasons for these discrepancies requires further effort, as they are linked to potential errors in wind speed (e.g. Marsham *et al.*, 2008), soil type and moisture and vegetative fraction.

These key results show the effectiveness of targeted intensive aircraft measurement campaigns like GERBILS in addressing problems in atmospheric observations and modelling. The detailed planning subsequent to the conception of the GERBILS project proved very valuable in effective deployment of the aircraft.

6. Future perspectives

GERBILS has provided many insights into the SW and LW radiative effects of mineral dust, our ability to quantitatively assess mineral dust loadings from space, and the accuracy of current global and mesoscale models in forecasting dust production, transport and deposition. However, it is worth considering how we can move forward in the future.

In situ measurements of large particles such as mineral dust pose considerable problems for instrumented aircraft. Coarse-mode mineral dust particles have been measured using FSSP instruments, which use only a very narrow range of forward scattering angles, that were originally developed for measuring small cloud droplets (e.g. Weinzierl *et al.*, 2009). However, recent research developments such as the SID-2 detector enable a more robust assessment of the physical properties of mineral dust as the size and non-sphericity of the particles can be simultaneously assessed (Johnson and Osborne, 2011). Also, probes such as the Cloud, Aerosol and Precipitation Spectrometer (CAPS, http://www.dropletmeasurement.com/) extend the range of radii that can be measured from that of the PCASP-100X, which measures accumulation mode aerosols. To definitively determine the accuracy of measurements of the coarse mode and corrections made in calibrating the instruments, wing-tip to wing-tip measurements in dusty environments over AERONET sun photometers should be performed.

Owing to the presence of a significant coarse mode, it has become widely appreciated that mineral dust exerts a significant impact on both the SW and LW fluxes in the atmosphere. At the top of the atmosphere the impact in cloud-free conditions is strongest for the SW over the ocean where the surface reflectance is lowest (e.g. Haywood *et al.*, 2011), while the impact is strongest for the LW over land where the surface skin temperature is highest (e.g. Osborne *et al.*, 2011; Haywood *et al.*, 2005). For the SW, the single scattering albedo determined from *in situ* and remote sensing measurements indicates relatively low absorption (mean SSA_{550} of 0.97) but the range of 0.92–0.99 suggests that absorption is variable by a factor of around three. This is not surprising as there will undoubtedly be regional variations owing to different mineral dust size distributions and chemical compositions. Although satellite remote sensing over desert surfaces has made significant progress by using either infra-red channels (e.g. Brindley and Russell, 2009) or by using UV channels where the surface reflection is invariant (e.g. Hsu *et al.*, 2006), a reliable method for determining the single scattering albedo from space would be a welcome addition. The use of underlying bright targets such as stratocumulus clouds may offer some ways forward (e.g. Haywood *et al.*, 2004), although the near-zero Ångström exponent associated with mineral dust and relatively low absorption would likely make smaller, more highly absorbing particles such as biomass-burning aerosols more suitable for such an approach.

The non-sphericity of mineral dust causes some considerable uncertainty in SW remote sensing retrievals owing to variations in the scattered radiance. While a number of models have been developed based on measurements of the forward-scattered radiance from AERONET observations (e.g. Dubovik *et al.*, 2006) the applicability of these models for backscattered radiances should be further tested. The Aerosol Polarimetry Sensor (APS) on the GLORY mission may assist in this regard (http://glory.giss.nasa.gov/aps) would have assisted in this regard as radiances and polarised radiances would have been measured over a wide range of scattering angles, but unfortunately the satellite failed to gain orbit on launch.

While SEVIRI retrievals using infra-red channels have led to some significant steps forward in remote sensing over both ocean and land at high temporal frequency, only a few spectral channels are used. Fully spectrally resolved LW features at high spectral resolution can be derived using the aircraft-mounted ARIES interferometer (Haywood *et al.*, 2011; Osborne *et al.*, 2011). This approach could be made global using new satellite retrievals which are being developed using the Infrared Atmospheric Sounding Instrument (IASI). These will allow a comprehensive assessment of the variability of refractive indices in the atmospheric window and allow greater confidence in assessments of the LW impacts.

Dust modelling has made significant steps forward in the past decade, with NWP global and mesoscale models able to represent dust storms driven by larger synoptic features. However, modelling dust outbreaks driven by smaller-scale cold pools from convective downdrafts remains a challenging issue. Model resolution will need to improve considerably so that the intense gust fronts associated with convective downdrafts are accurately represented before dust generation at relatively local scales can be resolved (e.g. Reinfreid *et al.*, 2009). This approach is currently impractical in coarse-resolution global models; development of parameterisations utilising sub-grid-scale probability distribution functions of wind speed in dust generation could give some benefits. From a climate forcing and climate feedback point of view, determination of the anthropogenic fraction of mineral dust is an ill-defined problem (Forster *et al.*, 2007) as increased dust generation can be via increased grazing (technically a forcing) or via increased desertification from warming and drying (technically a feedback). Only by utilising models can such processes be elucidated.

Acknowledgements

Airborne data were obtained using the BAe-146-301 Atmospheric Research Aircraft (ARA) flown by Direct flight Ltd and managed by the Facility for Airborne Atmospheric Measurements (FAAM), which is jointly funded by the Met Office and the Natural Environment Research Council (NERC). The staff of the Met Office, FAAM, Direct flight and Avalon engineering are thanked for their dedication in making the GERBILS measurement campaign a success.

References

Allan RP, Slingo A, Milton SF, Culverwell I. 2005. Exploitation of Geostationary Earth Radiation Budget data using simulations from a numerical weather prediction model: methodology and data validation. *J. Geophys. Res.* **110**: D14111, DOI: 10.1029/2004JD005698.

Allan RP, Woodage MJ, Milton SF, Brooks MA, Haywood JM. 2011. Examination of longwave radiative bias in general circulation models over north Africa during May–July. *Q. J. R. Meteorol. Soc.* **137**: 1179–1192, DOI: 10.1002/qj.717 (this issue).

Anderson TL, Ogren JA. 1998. Determining aerosol radiative properties using the TSI 3563 integrating nephelometer. *Aerosol Sci. Technol.* **29**: 57–69.

Andreae MO, Berresheim H, Andreae TW, Kritz MA, Bates TS, Merrill JT. 1998. Vertical distribution of dimethylsulfide, sulfur dioxide, aerosol ions, and radon over the northeast Pacific Ocean. *J. Atmos. Chem.* **6**: 149–173.

Balkanski Y, Schulz M, Claquin T, Guibert S. 2007. Reevaluation of mineral aerosol radiative forcings suggests a better agreement with satellite and AERONET data. *Atmos. Chem. Phys.* **7**: 81–95.

Bond TC, Anderson TL, Campbell D. 1999. Calibration and intercomparison of filter-based measurements of visible light absorption by aerosols. *Aerosol Sci. Technol.* **30**: 582–600.

Brindley H, Russell J. 2008. Assessing the errors in shortwave radiative fluxes inferred from the Geostationary Earth Radiation Budget (GERB) instrument in the presence of dust aerosol. *J. Appl. Meteorol.* **47**: 1659–1680.

Brindley H, Russell J. 2009. An assessment of Saharan dust loading and the corresponding cloud-free longwave direct radiative effect from geostationary satellite observations. *J. Geophys. Res.* **114**: D23201, DOI:10.1029/2008JD011635.

Capes G, Johnson B, McFiggans G, Williams PI, Haywood JM, Coe H. 2008. Aging of biomass burning aerosols over West Africa: aircraft measurements of chemical composition, microphysical properties, and emission ratios. *J. Geophys. Res.* **113**: D00C15, DOI: 10.1029/2008JD009845.

Chou C, Formenti P, Maille M, Ausset P, Helas G, Harrison M, Osborne S. 2008. Size distribution, shape, and composition of mineral dust aerosols collected during the African Monsoon Multidisciplinary Analysis Special Observation Period 0: Dust and Biomass-Burning Experiment field campaign in Niger, January 2006. *J. Geophys. Res.* **113**: D00C10, DOI: 10.1029/2008JD009897.

Christopher SA, Gupta P, Haywood J, Greed G. 2008. Aerosol optical thicknesses over North Africa. 1. Development of a product for model validation using Ozone Monitoring Instrument, Multiangle Imaging Spectroradiometer, and Aerosol Robotic Network. *J. Geophys. Res.* **113**: D00C04, DOI: 10.1029/2007JD009446.

Christopher SA, Gupta P, Johnson B, Brindley H, Haywood J, Hsu C. 2011. Multi-sensor satellite remote sensing of dust aerosols over North Africa during GERBILS. *Q. J. R. Meteorol. Soc.* **137**: 1168–1178, DOI: 10.1002/qj.863 (this issue).

Christopher SA, Johnson B, Jones TA, Haywood J. 2009. Vertical and spatial distribution of dust from aircraft and satellite measurements during the GERBILS field campaign. *Geophys. Res. Lett.* **36**: L06806, DOI: 10.1029/2008GL037033.

Cotton R, Osborne SR, Ulanowski Z, Hirst E, Kaye PH, Greenaway RS. 2010. The ability of the Small Ice Detector (SID-2) to characterise cloud particle and aerosol morphologies obtained during flights of the FAAM BAe-146 research aircraft. *J. Atmos. Oceanic Technol.* **27**: 290–303.

Dubovik O, Sinyuk A, Lapyonok T, Holben BN, Mishchenko M, Yang P, Eck TF, Volten H, Munoz O, Veihelmann B, van der Zande WJ, Leon J-F, Sorokin M, Slutsker I. 2006. Application of spheroid models to account for aerosol particle nonsphericity in remote sensing of desert dust. *J. Geophys. Res.* **111**: D11208, DOI: 10.1029/2005JD006619.

Formenti P, Rajot JL, Desboeufs K, Chevaillier S, Caquineau S, Nava S, Gaudichet A, Journet E, Triquet S, Alfaro S, Chiari M, Haywood JM, Coe H, Highwood EJ. 2008. Regional variability of the composition of mineral dust from western Africa: results from the AMMA SOP0/DABEX and DODO field campaigns. *J. Geophys. Res.* **113**: D00C13, DOI: 10.1029/2008JD009903.

Forster P, Ramaswamy V, Artaxo P, Berntsen T, Betts R, Fahey D, Haywood JM, Lean J, Lowe D, Myhre G, Nganga J, Prinn R, Raga G, Schulz M, Van Dorland R. 2007. Changes in atmospheric constituents and in radiative forcing. In *Climate Change 2007: The Physical Science Basis. Contribution of Working Group I to the Fourth Assessment Report of the Intergovernmental Panel on Climate Change*, Solomon S, Qin D, Manning M, Chen Z, Marquis M, Avery KB, Tignor M, Miller HL (eds). Cambridge University Press: Cambridge, UK; 139–234.

Greed G, Haywood JM, Milton S, Keil A, Christopher S, Gupta P, Highwood EJ. 2008. Aerosol optical depths over North Africa. 2. Modeling and model validation. *J. Geophys. Res.* **113**: D00C05, DOI: 10.1029/2007JD009457.

Harries JE, Russell JE, Hanafin JA, Brindley HE, Futyan J, Rufus J, Kellock S, Matthews G, Wrigley R, Last A, Mueller J, Mossavati R, Ashmall J, Sawyer E, Parker D, Caldwell M, Allan PM, Smith A, Bates MJ, Coan B, Stewart BC, Lepine DR, Cornwall LA, Corney DR, Ricketts MJ, Drummond D, Smart D, Cutler R, Dewitte S, Clerbaux N, Gonzalez L, Ipe A, Bertrand C, Joukoff A, Crommelynck D, Nelms N, Llewellyn-Jones DT, Butcher G, Smith GL, Szewczyk ZP, Mlynczak PE, Slingo A, Allan RP, Ringer MA. 2005. The Geostationary Earth Radiation Budget (GERB) experiment. *Bull. Am. Meteorol. Soc.* **86**: 945–960.

Havemann S, Baran AJ. 2001. Extension of T-matrix to scattering of electromagnetic plane waves by non-axisymmetric dielectric particles: application to hexagonal ice cylinders. *J. Quant. Spectrosc. Radiat. Transf.* **70**: 139–158.

Haywood JM, Francis P, Osborne SR, Glew M, Loeb N, Highwood E, Tanré D, Myhre G, Formenti P, Hirst E. 2003. Radiative properties and direct radiative effect of Saharan dust measured by the C-130 aircraft during SHADE. 1. Solar spectrum. *J. Geophys. Res.* **108**(D18): 8577, DOI: 10.1029/2002JD002687.

Haywood JM, Osborne SR, Abel SJ. 2004. The effect of overlying absorbing aerosol layers on remote sensing retrievals of cloud effective radius and cloud optical depth. *Q. J. R. Meteorol. Soc.* **130**: 779–800.

Haywood JM, Allan RP, Culverwell I, Slingo A, Milton S, Edwards JM, Clerbaux N. 2005. Can desert dust explain the outgoing longwave radiation anomaly over the Sahara during July 2003? *J. Geophys. Res.* **110**: D05105, DOI: 10.1029/2004JD005232.

Haywood JM, Pelon J, Formenti P, Bharmal N, Brooks M, Capes G, Chazette P, Chou C, Christopher S, Coe H, Cuesta J, Derimian Y, Desboeufs K, Greed G, Harrison M, Heese B, Highwood EJ, Johnson B, Mallet M, Marticorena B, Marsham J, Milton S, Myhre G, Osborne SR, Parker DJ, Rajot J-L, Schulz M, Slingo A, Tanré D, Tulet P. 2008. Overview of the African Multidisciplinary Monsoon Analysis Special Observational Period-0 and the Dust and Biomass burning Experiment. *J. Geophys. Res.* **113**: D00C17, DOI: 10.1029/2008JD010077.

Haywood JM, Johnson BT, Osborne SR, Mulcahy J, Brooks ME, Harrison MAJ, Milton SF, Brindley HE. 2011. Observations and modelling of the solar and terrestrial radiative effects of Saharan dust: a radiative closure case-study over oceans during the GERBILS campaign. *Q. J. R. Meteorol. Soc.* DOI: 10.1002/qj.770 (this issue).

Hesse E. 2008. Modelling diffraction during ray-tracing using the concept of energy flow lines. *J. Quant. Spectrosc. Radiat. Transf.* **109**: 1374–1383.

Highwood EJ, Haywood JM, Silverstone MD, Newman SM, Taylor JP. 2003. Radiative properties and direct effect of Saharan dust measured by the C-130 aircraft during SHADE. 2. Terrestrial spectrum. *J. Geophys. Res.* **108**(D18): 8578, DOI: 10.1029/2002JD002552.

Holben BN, Eck TF, Slutsker I, Tanr D, Buis JP, Setzer A, Vermote E, Reagan JA, Kaufman YJ, Nakajima T, Lavenu F, Jankowiak I, Smirnov A. 1998. AERONET: a federated instrument network and data archive for aerosol characterization. *Remote Sens. Environ.* **66**: 1–16.

Hsu NC, Tsay S-C, King MD, Herman JR. 2006. Deep blue retrievals of Asian aerosol properties during ACE-Asia. *IEEE Trans. Geosci. Remote Sens.* **44**: 3180–3195.

Johnson BT, Osborne SR. 2011. Physical and optical properties of mineral dust aerosol measured by aircraft during the GERBILS campaign. *Q. J. R. Meteorol. Soc.* **137**: 1117–1130, DOI: 10.1002/qj.777 (this issue).

Johnson BT, Christopher S, Haywood JM, Osborne SR, McFarlane S, Hsu C, Salustro C, Kahn R. 2009. Measurements of aerosol properties from aircraft, satellite and ground-based remote sensing: a case study from the Dust and Biomass burning Experiment (DABEX). *Q. J. R. Meteorol. Soc.* **135**: 922–934.

Johnson BT, Brooks ME, Walters D, Woodward S, Christopher S, Schepanski K. 2011. Assessment of the Met Office dust forecast model using observations from the GERBILS campaign. *Q. J. R. Meteorol. Soc.* **137**: 1131–1138, DOI: 10.1002/qj.736 (this issue).

Kahn RA, Gaitley BJ, Martonchik JV, Diner DJ, Crean KA, Holben B. 2005. Multiangle Imaging Spectroradiometer (MISR) global aerosol optical depth validation based on 2 years of coincident Aerosol Robotic Network (AERONET) observations. *J. Geophys. Res.* **110**: D10S04, DOI: 10.1029/2004JD004706.

Kandler K, Schutz L, Deutscher C, Ebert M, Hofmann H, Jackel S, Jaenicke R, Knippertz P, Lieke K, Massling A, Petzold A, Schladitz A, Weinzierl B, Wiedensohler A, Zorn S, Weinbruch S. 2009. Size distribution, mass concentration, chemical and mineralogical composition and derived optical parameters of the boundary layer aerosol at Tinfou, Morocco, during SAMUM 2006. *Tellus B* **61**: 32–50.

Kaufman YJ, Tanré D, Remer LA, Vermote EF, Chu A, Holben BN. 1997. Operational remote sensing of tropospheric aerosol over land from EOS moderate resolution imaging spectroradiometer. *J. Geophys. Res.* **102**: 17051–17068.

Klaver A, Formenti P, Caquineau S, Chevaillier S, Ausset P, Calzolai G, Osborne S, Johnson B, Harrison M, Dubovik O. 2011. Physico-chemical and optical properties of Sahelian and Saharan mineral dust: *in situ* measurements during the GERBILS campaign. *Q. J. R. Meteorol. Soc.* **137**: 1193–1210, DOI:10.1002/qj.889 (this issue).

Kokhanovsky AA. 2003. Optical properties of irregularly shaped particles. *J. Phys. D – Appl. Phys.* **36**: 915–923.

Lebel T, Parker DJ, Flamant C, Bourles B, Marticorena B, Mougin E, Peugeot C, Diedhiou A, Haywood JM, Ngamini JB, Polcher J, Redelsperger J-L, Thorncroft CD. 2010. The AMMA field campaigns: multiscale and multidisciplinary observations in the West African region. *Q. J. R. Meteorol. Soc.* **136**(S1): 8–33.

Marsham JH, Parker DJ, Grams CM, Taylor CM, Haywood JM. 2008. Uplift of Saharan dust south of the intertropical discontinuity. *J. Geophys. Res. (Atmos.)* **113**(D12): D21102, DOI: 10.1029/2008JD009844.

Milton SF, Greed G, Brooks ME, Haywood J, Johnson B, Allan RP, Slingo A, Grey WMF. 2008. Modeled and observed atmospheric radiation balance during the West African dry season: role of mineral dust, biomass burning aerosol, and surface albedo. *J. Geophys. Res.* **113**: D00C02, DOI: 10.1029/2007JD009741.

Osborne SR, Johnson BT, Haywood JM, Baran AJ, Harrison MAJ, McConnell CL. 2008. Physical and optical properties of mineral dust aerosol during the Dust and Biomass-burning Experiment, *J. Geophys. Res.* **113**: D00C03, DOI: 10.1029/2007JD009551.

Osborne SR, Baran AJ, Johnson BT, Haywood JM, Hesse E, Newman S. 2011. Short-wave and long-wave radiative properties of Saharan dust aerosol. *Q. J. R. Meteorol. Soc* **137**: 1149–1167, DOI: 10.1002/qj.771 (this issue).

Parker DJ, Burton RR, Diongue-Niang A, Ellis RJ, Felton M, Taylor CM, Thorncroft CD, Bessemoulin P, Tompkins AM. 2005. The diurnal cycle of the West African monsoon circulation. *Q. J. R. Meteorol. Soc.* **131**: 2839–2860.

Reinfried F, Tegen I, Heinold B, Hellmuth O, Schepanski K, Cubasch U, Huebener H, Knippertz P. 2009. Simulations of convectively driven density currents in the Atlas region using a regional model: impacts on dust emission and sensitivity to horizontal resolution and convection schemes. *J. Geophys. Res.* **114**: D08127, DOI: 10.1029/2008JD010844.

Remer LA, Kaufman YJ, Tanré D, Mattoo S, Chu DA, Martins JV, Li R-R, Ichoku C, Levy RC, Kleidman RG, Eck TF, Vermote E. 2005. The MODIS aerosol algorithm, products and validation. *J. Atmos. Sci.* **62**: 947–973.

Schladitz A, Müller T, Kaaden N, Massling A, Kandler K, Ebert M, Weinbruch S, Deutscher C, Wiedensohler A. 2009. In situ measurements of optical properties at Tinfou (Morocco) during the Saharan Mineral Dust Experiment SAMUM 2006. *Tellus* **61B**: 64–78.

Slingo A, Ackerman TP, Allan RP, Kassianov EI, McFarlane SA, Robinson GJ, Barnard JC, Miller MA, Harries JE, Russell JE, Dewitte S. 2006. Observations of the impact of a major Saharan dust storm on the atmospheric radiation balance. *Geophys. Res. Lett.* **33**: L24817, DOI: 10.1029/2006GL027869.

Tanré D, Haywood JM, Pelon J, Léon JF, Chatenet B, Formenti P, Francis P, Goloub P, Highwood EJ, Myhre G. 2003. Measurement and modeling of the Saharan dust radiative impact: overview of the SaHAran Dust Experiment (SHADE). *J. Geophys. Res.* **108**(D13): 8574, DOI: 10.1029/2002JD003273.

Torres O, Tanskanen A, Veihelman B, Ahn C, Braak R, Bhartia PK, Veefkind P, Levelt P. 2007. Aerosols and surface UV products from Ozone Monitoring Instrument observations: an overview. *J. Geophys. Res.* **112**: D24S47, DOI: 10.1029/2007JD008809.

Weinzierl B, Petzold A, Esselborn M, Wirth M, Rasp K, Kandler K, Schütz L, Koepke P, Fiebig M. 2009. Airborne measurements of dust layer properties, particle size distribution and mixing state of Saharan dust during SAMUM 2006. *Tellus* **61B**: 96–117.

Woodage MJ, Slingo A, Woodward S, Comer RE. 2010. UK-HiGEM: simulations of desert dust and biomass burning aerosols with a high-resolution atmospheric GCM. *J. Clim.* **23**: 1636–1659.

World Climate Program (WCP). 1986. *A Preliminary Cloudless Standard Atmosphere for Radiation Computation*. World Meteorological Organisation: Geneva.